Published in final edited form as:
Arch Ophthalmol. 2012 September ; 130(9): 1184–1189. doi:10.1001/archophthalmol.2012.1117.

Clinical characteristics of a large choroideremia pedigree carrying a novel *CHM* mutation

Alex S. Huang, MD, PhD[1], **Leo A. Kim, MD, PhD**[1], and **Amani A. Fawzi, MD**[1,2]

[1]Doheny Eye Institute, and Department of Ophthalmology, Keck School of Medicine of the University of Southern California, Los Angeles, California

[2]Department of Ophthalmology, Northwestern University, Feinberg School of Medicine, Chicago, Illinois

Abstract

Objective—We describe a large family with a novel mutation in *CHM*.

Clinical Relevance—To demonstrate a novel *CHM* mutation that emphasizes severe posterior pole carrier phenotypes, age-related changes, and early choroideremia pathology.

Methods—Subjects were characterized using clinical examination, widefield fundus photography, widefield autofluorescence, and spectral domain optical coherence tomography. The *CHM* mutation was identified with the NIH-sponsored eyeGene™ program.

Results—A novel nonsense *CHM* mutation (*T*1194*G*), resulting in a premature stop (Y398X) and loss of the final one-third C-terminal portion of the protein, was identified. A large pedigree was generated from information provided by the twice-married proband. Seven males (ages 27–39) and seven females (ages 22–89) were evaluated. Affected males showed characteristic peripheral chorioretinal atrophy with islands of macular sparing. Female carriers exhibited a wide range of variability, from mild pigmentary alterations to significant chorioretinal atrophy with severe vision loss. Older women tended to have a more severe phenotype. Autofluorescence demonstrating subfoveal loss or absence of RPE correlated with vision loss in both sexes. Spectral domain optical coherence tomography demonstrated dynamic remodeling over time of the outer retina including focal thickening, drusen-like deposits, and disruption to photoreceptor inner segment/outer segment junctions in young female carriers.

Conclusions—*CHM* (*T*1194*G*) is a novel mutation manifesting a wide range of phenotypic variability in a single family, with a trend toward more severe phenotypes in older female carriers. Our findings emphasize the importance of considering X-linked diseases and carefully evaluating pedigrees with severe pathology in females.

Choroideremia is an X-linked disorder typically presenting with progressive vision and visual field loss in middle-aged men. Fundoscopic examination shows scalloped areas of retinal pigment epithelium (RPE) and choroid loss (1, 2). Histologic evaluation shows pathological damage to RPE, choroid, and photoreceptors (2).

The *CHM* gene (Xq21.2) is responsible for choroideremia (3). It encodes a 653-amino acid protein, Rab escort protein 1 (REP1), which is localized to rod photoreceptor inner segments (4) and functions in vesicular transport through its interaction with RAB GTPases (Rabs) (1, 5–8). Although numerous mutations have been identified in this 15-exon gene, including

Correspondence: Amani A. Fawzi, MD, Department of Ophthalmology, Northwestern University, Feinberg School of Medicine, 645 N. Michigan Ave, Suite 440, Chicago, Illinois 60611, AFawzimd@gmail.com.

deletions, translocations, missense mutations, nonsense mutations, and splice-site mutations (3, 8–11), genotype/phenotype relationships have been difficult to establish (12).

Whereas young affected males present with peripheral scalloped chorioretinal lesions that tend to spare the posterior pole in the later stages of the disease, female carriers typically show subtle retinal peripheral pigmentary changes (5, 13, 14). Female carriers are technically heterozygous; however, lyonization of the X chromosome in each somatic cell results in a mosaic pattern of cells across the body in which each cell preferentially expresses either the maternal or paternal X chromosome. Genetic evidence exists that *CHM* can partially escape X inactivation (15). The presence of varying levels of small REP-1 transcripts through this mechanism may allow for potentially greater variability in the manifestation of choroideremia in female carriers (5, 13).

Here we describe a family with a novel nonsense *CHM* mutation (*T*1194*G*), resulting in a premature stop (Y398X). This mutation was uncovered in a female proband presenting with severe choroideremia carrier findings. Pedigree construction identified two families, linked by the twice-married proband, demonstrating a wide range of phenotypic severity in choroideremia carriers. The patients were systematically evaluated using widefield photography, widefield autofluorescence, and spectral domain optical coherence tomography (OCT). This family and their novel mutation (*T*1194*G*) are important as their range of phenotypic variability sheds light on age-related and early changes in choroideremia carriers.

Methods

All patients were examined at the Doheny Eye Institute from February 2010 to March 2011. The research protocol was approved by the Institutional Review Board of the University of Southern California and was in accordance with the tenets set forth in the Declaration of Helsinki. All subjects were informed of the purpose of the examination, volunteered, and signed a written, informed consent prior to examination and phlebotomy. Ophthalmic examination included best-corrected visual acuity (BCVA), slit-lamp biomicroscopy, and dilated fundus exam. A family history was taken and a pedigree was created. Genotyping was performed on blood samples submitted to the NIH-sponsored eyeGene™ program for 12 of the 14 patients.

All patients underwent widefield fundus photography (pseudo-color red/green) and fundus autofluorescence (green-light; wavelength 532 nm) using the Optos 200Tx scanning laser ophthalmoscope (Optos PLC, Dunfermline, UK). The female proband and selected female carriers underwent OCT in registration with cSLO infrared reflectance images (793 nm) and cSLO autofluorescence (488 nm) images using Spectralis HRA+OCT (Heidelberg Engineering, Heidelberg, Germany). To compare the same areas of the retina across time, registered infrared images obtained at baseline served as a reference for future OCT images. The cSLO autofluorescence images were manually overlaid onto infrared images using the retina vessels and optic nerve as invariable landmarks to obtain pseudo-registration of autofluorescence with OCT images.

Results

The proband is an 89-year-old Hispanic female who was referred for evaluation of a degenerative retinal disorder. Past ocular history was significant for poor vision requiring spectacles in her 20s, subsequent gradual vision decline, and cataract extraction with intraocular lens placement in the right eye, without visual improvement. The patient's distance BCVA measured 20/400 and 20/200 in the right and left eyes, respectively. Careful

discussion with the proband (II:3) revealed two large families resulting from her two marriages, with several offspring affected by visual problems (Table 1 and Figure 1). The proband had 16 children, many of whom had received a diagnosis of retinitis pigmentosa. Seven males (ages 27–39) and seven females (ages 22–89) were examined.

Molecular analysis revealed that the proband was heterozygous for a *T*1194*G* mutation in the *CHM* gene, resulting in a nonsense Y398X mutation. This mutation resulted in the truncation of the final one-third of the protein. All family members who were genotyped had the same mutation.

Clincal examination of the affected males (age 27–39) revealed scalloped areas of choroid/RPE loss typically seen in choroideremia (Figure 2). We correlated widefield fundus autofluorescence to vision by outlining the location of islands of preserved RPE (Figure 2). As such, most males had preservation of RPE subfoveally commensurate with BCVA of between 20/20 and 20/40. In one grandson (IV:2), whose BCVA was 20/100 in the left eye, autofluorescence showed a crescent-shaped remnant RPE island that was located outside the fovea.

Examination of female carriers identified a wide range of phenotypic variability. Older carriers, such as the proband (II:3) and a 61-year-old niece (III:1), demonstrated scalloped areas of RPE atrophy and choroid loss reminiscent of male choroideremia (Figure 3). Unlike findings in males, the atrophic areas in these female carriers were centered in the posterior pole rather than in the periphery. Widefield autofluorescence clearly demonstrated scalloped areas of RPE loss with variable islands of preserved intact RPE (Figure 3). Subfoveal atrophy explained their poor vision (ranging from 20/200 to HM). Optical coherence tomography of the proband showed outer retinal atrophy, choroidal thinning, and increased OCT signal transmission in the choroid, suggestive of RPE loss (Figure 4).

Younger female carriers, ranging in age from 22 to 48 years, demonstrated good central vision with a milder phenotype typical of choroideremia carriers (Figure 3). The oldest female (III:3) in the younger cohort showed the most severe of the mild phenotypes. Examination of her macula revealed clear pigmentary changes and irregularities in autofluorescence. Comparing fundus photography in younger and older carriers identified progressively more chorioretinal involvement with age. Older carriers also showed generalized decreased autofluorescence, with residual areas of autofluorescence disturbance representing RPE pathology (Figure 3).

Spectralis OCT of the female carriers demonstrated dynamic changes and remodeling over time. Areas of outer retinal thickening (Figure 5; arrows) and focal drusenoid RPE deposits (Figure 5; single/double asterisks) associated with inner segment/outer segment (IS/OS) loss were interspersed with areas of intact IS/OS and relatively normal external limiting membrane and RPE. Registration of OCT images to infrared reflectance images (which were manually registered to autofluorescence) allowed point-to-point comparison of abnormal areas on the OCT to autofluorescence images. The drusenoid deposits correlated with areas of hyper-autofluorescence (Figure 5; single/double asterisks in C/F). Furthermore, comparison with images of affected areas examined 1 year later showed remodeling over time. In some cases, the pathology increased (for example, a single drusenoid deposit doubled; Figure 5, comparing single asterisks in A/D and C/F). The focal outer segment deposits and elongated outer segments appeared, over time, to evolve into RPE thickening, leading to the appearance of RPE deposits, suggestive of underlying RPE dysfunction. These changes were corroborated by the autofluorescence changes. Other areas showed improvement, where the subretinal deposit disappear, with retention of relatively normal surrounding IS/OS junction and RPE (Figure 5; comparing double asterisks in B/E and C/F).

Discussion

To our knowledge, this is the first report of the *T*1194*G* mutation resulting in an Y398X premature stop in the *CHM* gene, a novel mutation that results in a wide range of phenotypic severity in female carriers. The findings in females range from typical pigmentary changes to more severe, scalloped atrophic changes that, unlike the atrophic changes in males, show a predilection toward the posterior pole (Figure 3). The posterior pole is also the main location of RPE changes in younger, more mildly affected female carriers (Figure 3). Males show characteristic scalloped atrophic choroideremia changes (Figure 2).

The *T*1194*G* mutation results in loss of the final one-third of the C-terminus of REP1. Most described mutations of *CHM* are nonsense mutations, splice error mutations, or frameshift mutations, leading to premature stop codons that result in an abnormal protein or no expression from nonsense-mediated decay (3, 7, 9–11). Rare missense mutations have been described, resulting in presumably misfolded and nonfunctional proteins (8, 16). While no clear genotype/phenotype correlation exists (eg. patients in whom the entire choroideremia *CHM* gene is missing do not necessarily have worse phenotypes (17)), a limited structure/function understanding of the CHM protein does identify critical residues. CHM shares significant sequence similarities with the guanine nucleotide dissociation inhibitor family identifying two important sequence conserved regions (SCRs) for Rab binding (7, 8). Crystal structure analysis of a Rab7:Rep1 complex also identifies a critical C-terminus mobile lid that coordinates Rab:Rep binding (18). This agrees with earlier observations that recombinant REP1 lacking the final 70 amino acids cannot mediate geranylgeranylation with geranylgeranyl transferase II, which is critical for Rab membrane attachment (9, 10). The premature stop seen in the *T*1194*G* mutation is downstream of the SCRs and thus spares them. However, the *T*1194*G* mutation does result in absence of the critical C-terminus domain. Therefore, the significance of the *T*1194*G* mutation is manifested either though a truncated protein product without the critical C-terminus or through nonsense-mediated decay.

Without clear genotype/phenotype correlation, an argument for a skewed pattern of X-chromosome inactivation in female carriers is typically used to explain phenotypic variation (5, 13, 14). While this is a reasonable concept, experimental demonstration of asymmetric X-inactivation in *CHM* has been complicated and elusive. Attempts to demonstrate asymmetric X-inactivation in two Mexican cohorts did not show skewed X-inactivation in one family and showed paradoxical skewed X-inactivation away from the mutated *CHM* in another family (19). Of course, this study was conducted using isolated peripheral whole blood leukocytes, and the authors acknowledged that any peripheral asymmetric X-inactivation may not necessarily reflect X-inactivation in the eyes. Furthermore, studies using primary female fibroblast cell lines suggested that human cells can undergo bi-allelic expression of *CHM*, implying the possibility of partial X-inactivation escape for *CHM* (15). Ultimately, the best insight into X-inactivation in choroideremia may be gained by studying chorioretinal tissue from carriers.

The *T*1194*G* pedigree showed high intrafamilial phenotypic variability, especially among females. Rare cases of severe choroideremia carriers have been described, and their presence is thought to be due to asymmetric X-inactivation (5, 13, 14). While some reports support an increased prevalence of skewed X-inactivation beyond the age of 30 (20), the range and rate of variability in females of the *T*1194*G* family may point toward more than just random X-inactivation. The trend of progressively worse phenotypes with advancing age argues against a random event causing some women to be severely affected while others are only mildly affected. A relationship between age and disease progression in choroideremia carriers is in agreement with some (13, 21, 22) but not all reports in the literature (23). There

are several potential reasons for this controversy. Many of the previous studies measured the rate of progression in carriers based on vision rather than on retinal changes. Most choroideremia carriers do not progress to the advanced level of disease seen amongst carriers in this series, in whom visual acuity is affected. The use of vision to define progression in carriers may have lead these authors to underestimate the age-related changes; most carriers retain excellent vision and remain asymptomatic despite the progression of RPE changes. By virtue of the wide range of ages and phenotypes in the carriers reported herein, we identified a pattern of worse phenotype with advancing carrier age, which may point toward complicated mechanisms (environmental or epigenetic) by which a REP1 mutation modifies the manifestations of the choroideremia disease. To confirm this hypothesis, long–term follow up of disease progression in young female carriers in this pedigree will be important to evaluate whether these carriers eventually exhibit clinical features seen in the older female carriers.

The primary cellular site of the pathologic changes in choroideremia continues to be an active area of research. The name of the disease implies that the choroid and its vasculature is the site of disease onset, with secondary damage to adjacent structures. However, this has been disputed by findings in mutant mouse models of choroideremia, where histopathology shows early damage to retina and RPE (9, 24, 25). While mild inflammation has been observed in the choroid at the junction of normal and atrophic retina in affected males (2), most studies point toward the RPE (26) or retina (4) as the site of disease onset. Examination of the edge of atrophic areas in affected men, using topographic analysis and laminar reflectivity patterns of raster time domain-OCT, suggested that retinal thickening precedes or coincides with photoreceptor abnormalities as the earliest finding, followed by outer retinal atrophy and loss of lamination (27). Our examination of young, mildly affected carriers with the *T*1194*G* mutation allowed us to explore early changes in choroideremia and to show similar findings.. Areas of outer retinal thickening and drusen-like deposits occur near areas of IS/OS segment disruption. Point-to-point correlation of autofluorescence to OCT in carrier females identified hyper-autofluorescent areas co-localizated with the drusen-like deposits and RPE thickening on OCT. This may reflect the accumulation of indigestible autofluorescent material, such as photoreceptor outer segments, leading to enlargement of RPE cells. Regardless of the exact sequence of disease onset, whether in the RPE or photoreceptors, early changes in choroideremia are clearly dynamic, as evidenced by the OCT findings. Registered areas of the retina showed either improvement or worsening of abnormalities over time (Figure 5).

In conclusion, *T*1194*G* is a novel mutation in *CHM* leading to the loss of the final one-third of REP1. The mutation identified in this family is important as it may be associated with a more severe, age-dependent phenotype in female carriers and may implicate more complicated mechanisms for choroideremia disease expression or age-related skewed X-inactivation. Our analysis of the mild female carriers also implied that the retinal photoreceptors or RPE may be the primary site of disease onset. Importantly, findings in this large family suggest that clinicians need to consider X-linked diseases even when severe pathology is seen in females, such as in cases of choroidal sclerosis (28), In these cases, careful analysis of the pedigree is important to examine the possibility of X-linked transmission.

Acknowledgments

The authors thank Martina Groeblacher, Susan Clarke, and Peter Mallen for assistance with figure preparation. Leo A. Kim is a Heed Fellow and receives support from the Heed Ophthalmic Foundation. This work is supported in part by Research to Prevent Blindness.

References

1. Seabra MC, Mules EH, Hume AN. Rab GTPases, intracellular traffic and disease. Trends in Molecular Medicine. 2002; 8(1):23–30. [PubMed: 11796263]
2. MacDonald IM, Russell L, Chan C. Choroideremia: New findings from ocular pathology and review of recent literature. Survey of ophthalmology. 2009; 54(3):401–7. [PubMed: 19422966]
3. van Bokhoven H, Schwartz M, Andreasson S, et al. Mutation spectrum in the *CHM* gene of danish and swedish choroideremia patients. Human Molecular Genetics. 1994; 3(7):1047–51. [PubMed: 7981671]
4. Syed N, Smith JE, John SK, Seabra MC, Aguirre GD, Milam AH. Evaluation of retinal photoreceptors and pigment epithelium in a female carrier of choroideremia. Ophthalmology. 2001; 108:711–20. [PubMed: 11297488]
5. Potter MJ, Wong E, Szabo SM, McTaggart KE. Clinical findings in a carrier of a new mutation in the *choroideremia* gene. Ophthalmology. 2004; 111:1905–9. [PubMed: 15465555]
6. Pereira-Leal JB, Hume AN, Seabra MC. Prenylation of rab GTPases: Molecular mechanisms and involvement in genetic disease. FEBS Letters. 2001; 498(2–3):197–200. [PubMed: 11412856]
7. Alory C, Balch WE. Organization of the rab-GDI/CHM superfamily: The functional basis for choroideremia disease. Traffic. 2001; 2:532–43. [PubMed: 11489211]
8. Sergeev YV, Smaoui R, Sui D, et al. The functional effect of pathogenic mutations in rab escort protein 1. Mutation Research. 2009; 665:44–50. [PubMed: 19427510]
9. van den Hurk, Jose AJM, Hendriks W, van de Pol TJR, et al. Mouse choroideremia gene mutation causes photoreceptor cell degeneration and is not transmitted through the female germline. Human Molecular Genetics. 1997; 6:857–8.
10. van den Hurk, Jose AJM, Schwartz M, van Bokhoven H, et al. Molecular basis of choroideremia (CHM): Mutations involving the rab escort protein-1 (REP-1) gene. Human Mutation. 1997; 9:110–7. [PubMed: 9067750]
11. Itabashi I, Wada Y, Kawamura M, Sato H, Tamai M. Clinical features of japanese families with a 402DelT or a 555–556DelAG mutation in choroideremia gene. Retina. 2004; 24:940–5. [PubMed: 15579993]
12. Hayakawa M, Fujiki K, Hotta Y, et al. Visual impairment and REP-1 gene muations in japanese choroideremia patients. Ophthalmic Genetics. 1999; 20:107–15. [PubMed: 10420196]
13. Renner AB, Fiebig BS, Cropp E, Weber BHF, Kellner U. Progression of retinal pigment epithelial alternations during long-term follow-up in female carriers of choroideremia and report of a novel *CHM* mutation. Archives of Ophthalmology. 2009; 127(7):907–12. [PubMed: 19597113]
14. Renner AB, Kellner U, Cropp E, et al. Choroideremia: Variability of clinical and electrophysiological characteristics and first report of a negative electroretinogram. Ophthalmology. 2006; 113:2066–73. [PubMed: 16935340]
15. Carrel L, Willard HF. Heterogeneous gene expression from the inactive X chromosome: An X-linked gene that escapes X inactivation in some human cell lines but is inactivated in other. Proceedings of the National Academy of Sciences USA. 1999; 96:7364–9.
16. Donnelly P, Menet H, Fouanon C, et al. Missense mutation in the choroideremia gene. Human Molecular Genetics. 1994; 3(6):1017. [PubMed: 7951216]
17. Mura M, Sereda C, Jablonski MM, MacDonald IM, Iannaccone A. Clinical and functional findings in choroideremia due to complete deletion of the *CHM* gene. Archives of Ophthalmology. 2007; 125(8):1107–13. [PubMed: 17698759]
18. Rak A, Pylypenko O, Niculae A, Pyatkov K, Goody RS, Alexadrov K. Structure of the Rab7:REP-1 complex: Insights into the mechanism of rab prenylation and choroideremia disease. Cell. 2004; 117:749–60. [PubMed: 15186776]
19. Perez-Cano HJ, Garnica-Hayashi RE, Zenteno JC. *CHM* gene molecular analysis and X-chromosome inactivation pattern determination in two families with choroideremia. American Journal of Medical Genetics. 2009; 149:2134–40. [PubMed: 19764077]
20. Hatakeyama C, Anderson CL, Beever CL, Penaherrera MS, Brown CJ, Robinson WP. The dynamics of X-inactivation skewing as women age. Clinical Genetics. 2004; 66:327–32. [PubMed: 15355435]

21. Roberts MF, Fishman GA, Roberts DK, et al. Retrospective, longitudinal, and cross sectional study of visual acuity impairment in choroideraemia. Br J Ophthalmol. 2002; 86:658–62. [PubMed: 12034689]

22. Rudolph G, Preising MN, Kalpadakis P, Haritoglou C, Lang GE, Lorenz B. Phenotypic variability in three carriers from a family with choroideremia and a frameshift mutation 1388delCCinsG in the REP-1 gene. Ophthalmic Genetics. 2003; 24:203–14. [PubMed: 14566650]

23. Coussa, R.; Kim, J.; Traboulsi, E. ARVO. Fort Lauderdale; Florida: May 4. 2011 Choroideremia: A meta analysis of the disease course.

24. Tolmachova T, Anders R, Abrink M, et al. Independent degeneration of photoreceptors and retinal pigment epithelium in conditional knockout mouse models of choroideremia. The Journal of Clinical Investigation. 2006; 2:386–94. [PubMed: 16410831]

25. Bonilha VL, Trzupek KM, Li Y, et al. Choroideremia: Analysis of the retina from a female symptomatic carrier. Ophthalmic Genetics. 2008; 29:99–110. [PubMed: 18766988]

26. Flannery JG, Bird AC, Farber DB, Weleber RG, Bok D. A histopathologic study of a choroideremia carrier. Investigative ophthalmology and visual science. 1990; 31–32:229–36.

27. Jacobson SG, Cideciyan AV, Sumaroka A, et al. Remodeling of the human retina in choroideremia: Rab escort protien 1 (REP-1) mutations. Investigative ophthalmology and visual science. 2006; 47(9):4113–20. [PubMed: 16936131]

28. Hwang JC, Kim DY, Chou CL, Tsang SH. Fundus autufluorescence, optical coherence tomography and electroretinogram findings in choroidal sclerosis. Retina. 2010; 30:1095–103. [PubMed: 20224472]

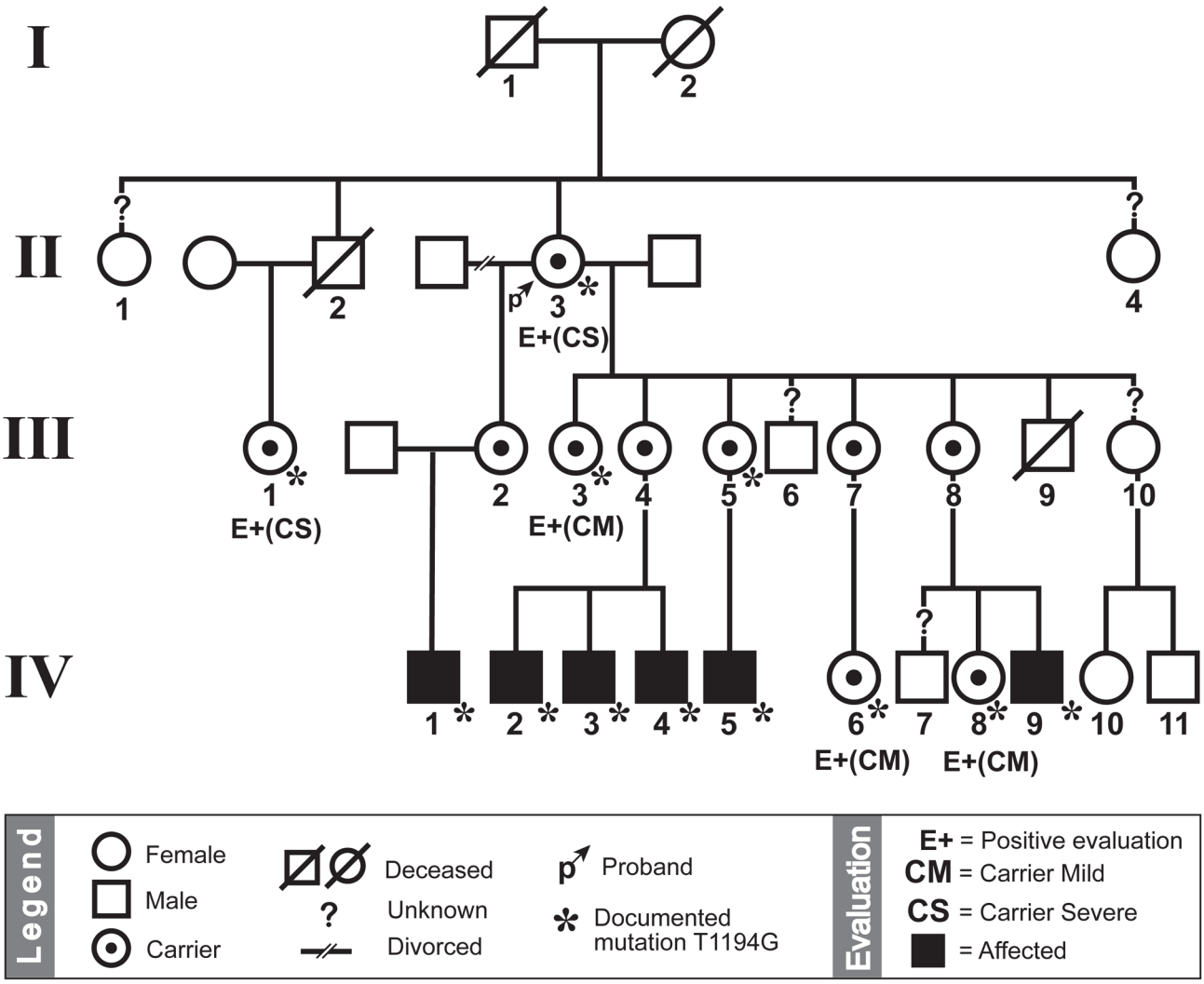

Figure 1.

The 89-year-old proband (II:3; arrow) married twice, generating two large pedigrees. Affected males are denoted by a filled square. Examined carrier females are denoted by (E+) and further subdivided into mild (CM) and severe (CS) based on clinical exam. All examined individuals within the family were genotyped except patients IV:10 and IV:11. Note that patients IV:10 and IV:11 demonstrated normal findings, implying that their mother (III:8) was not a carrier and inherited a normal X-chromosome from the proband.

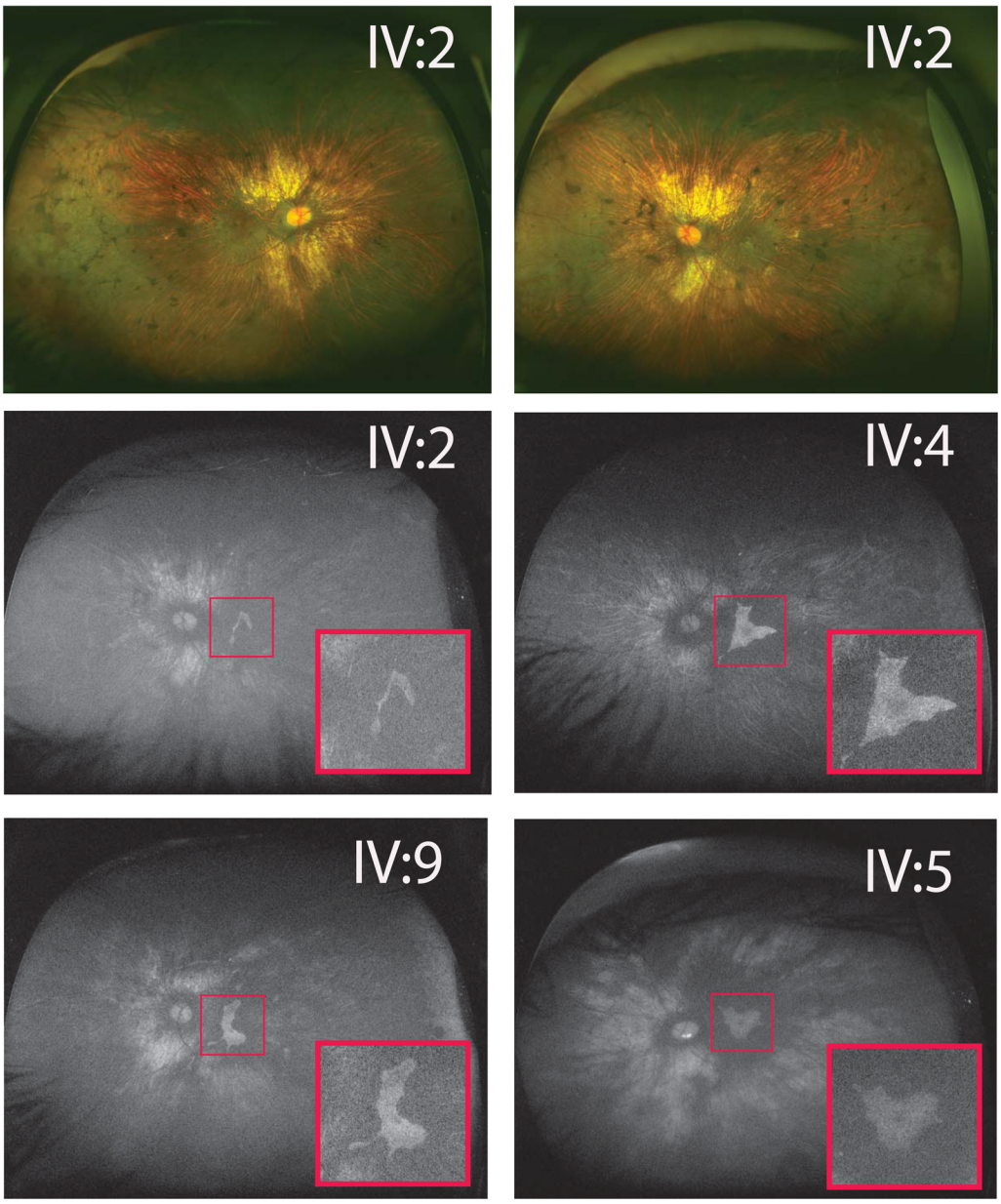

Figure 2.

Males showed typical choroideremia changes with scalloped retinal pigment epithelium (RPE)/choroid loss and areas of bare sclera. Bony spicules were seen in the periphery without waxy pallor of optic nerves or attenuated vessels. Widefield autofluorescence demonstrated areas of residual RPE (insets) in affected male left eyes. IV:2 image showed a small island of remaining autofluorescence, excluding the fovea, explaining his 20/100 vision. All other eyes depicted had between 20/20 and 20/25 vision. IV:5 showed an incidental finding of inferior optic nerve head drusen.

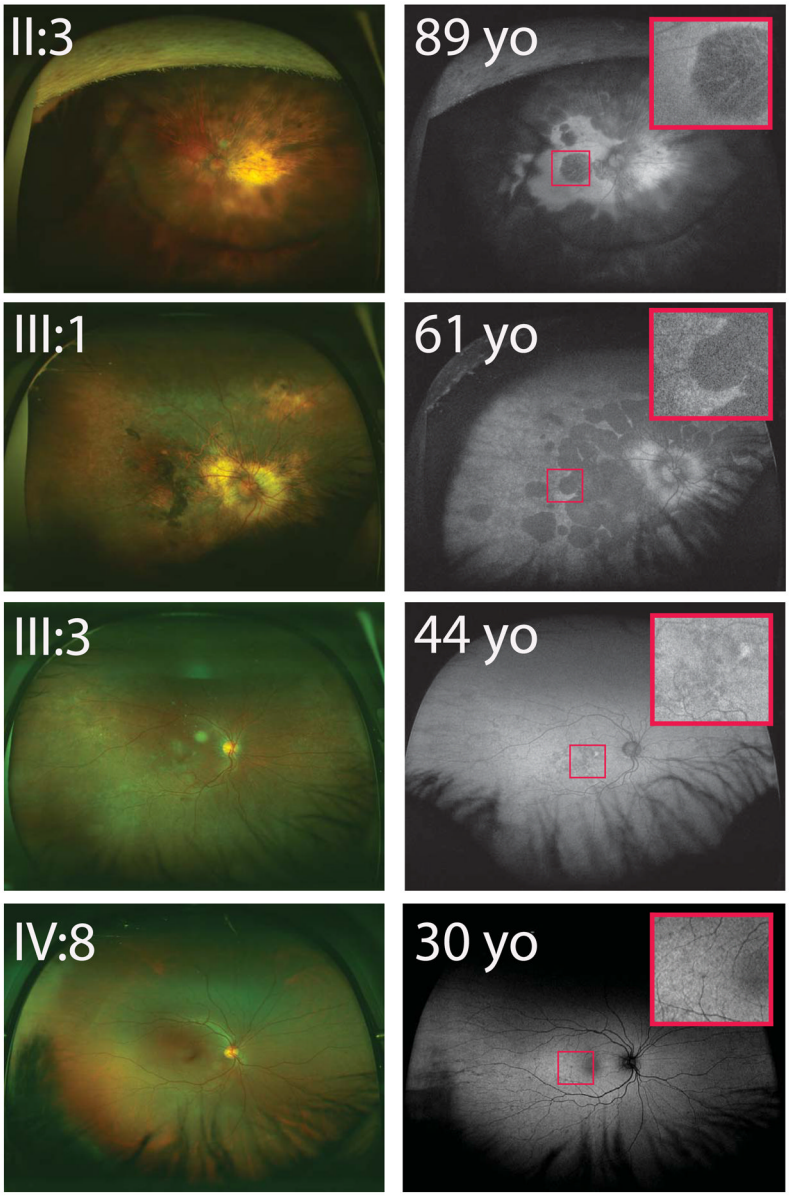

Figure 3.
Female carriers showed worsening phenotypes with age. Older, severe female carriers (II:3 & III:1) showed peripapillary choroid loss with bony spicule changes in the central and peripheral retina. Widefield autofluorescence demonstrated retinal pigment epithelial loss in a scalloped pattern with foveal involvement in both patients (insets). Younger and milder female carriers (III:3 & IV:8) appeared less affected, with relatively fewer macular autofluorescence irregularities (insets). All women depicted in this figure were confirmed to have the *T*1194*G* mutation.

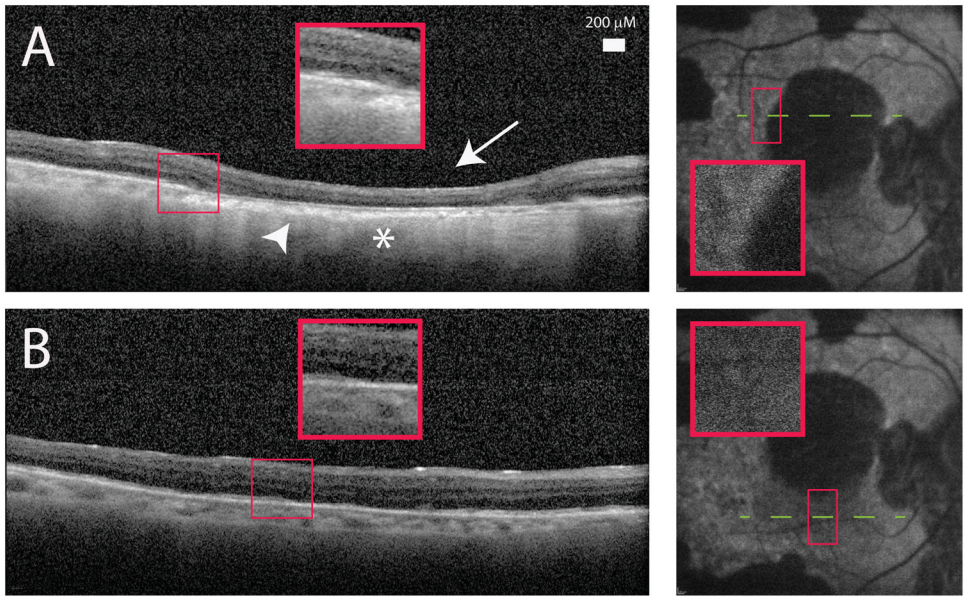

Figure 4.

A) Spectralis optical coherence tomography (OCT) image of the proband (II:3) showed outer retinal loss (arrow) and choroidal thinning (arrowhead). This area corresponded to absent blue autofluorescence as well as increased OCT signal transmission in the choroid indicative of retinal pigment epithelial loss (asterisk). B) Retinal areas with normal autofluorescence demonstrated improved retinal lamination and thicker choroid.

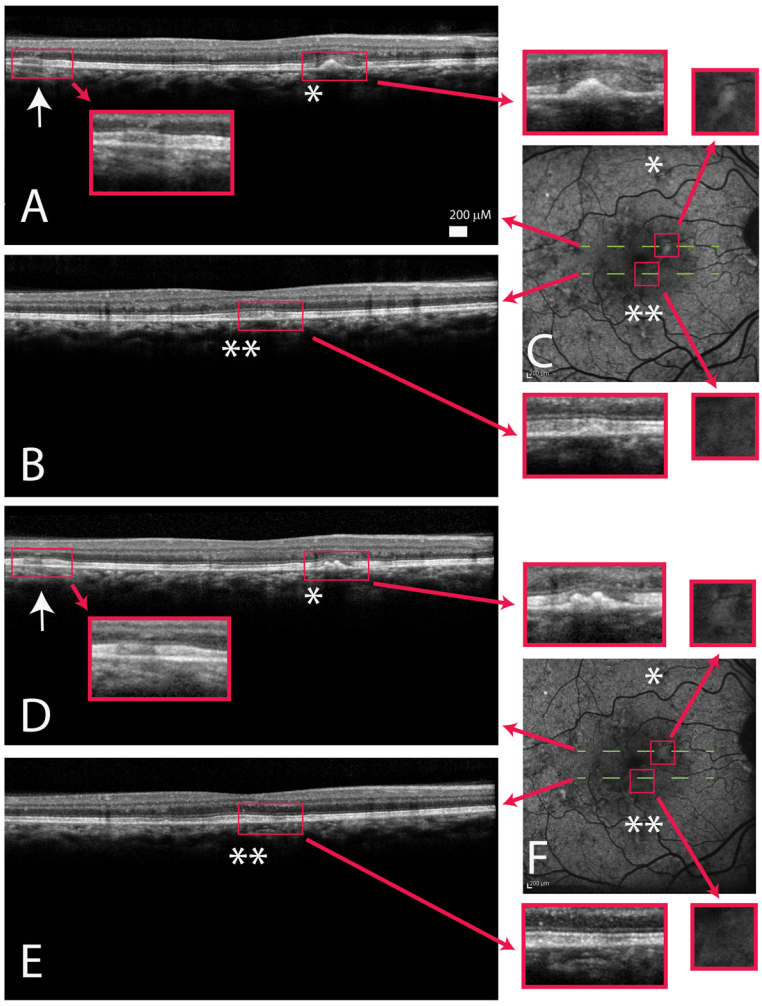

Figure 5.

A/B)Spectralis optical coherence tomography (OCT) image of a young female carrier (III:3) showed early outer retinal thickening (arrow) with focal retinal pigment epithelium hyper-reflective, drusen-like deposits (single/double asterisks) associated with the loss of the inner segment/outer segment junction. C)Autofluorescence images demonstrated macular irregularity and areas of drusen-like deposits that appeared hyper-autofluorescent. D/E)Spectralis OCT of III:3 one year later showed persistent outer retina thickening (D; arrow) and also dynamic changes with both worsening (comparing A/D asterisks) and improvement (comparing B/E double asterisks) of drusen-like material. Choroid and choriocapillaris appeared relatively normal. F)Autofluorescence obtained one year later showed increase in size of the drusen-like material correlating to an enlarged area of hyper-autofluorescence (comparing top line C/F) and resolution of the drusen-like material corresponding to a lessening of hyper-autofluorescence (comparing bottom line C/F). Red arrows showed enlarged images of highlighted areas.

Table 1

Genotype positive carrier females are arranged by descending age. All males have good vision except IV:2 who showed RPE loss involving the fovea OS. IV:10 and IV:11 were examined but not genetically tested (NT: not tested).

Patient	Sex	Age	*T1194G*	Vision (OD;OS)	Findings
II:3	F	89	+	20/400;20/200	Diffuse scalloped retina/RPE atrophy with pigment clumping
III:1	F	61	+	HM;HM	Diffuse scalloped retina/RPE atrophy with pigment clumping
III:5	F	48	+	20/20;20/25	Moderate macular RPE changes and autofluorescence irregularities
III:3	F	44	+	20/20;20/20	Moderate macular RPE changes and autofluorescence irregularities
IV:8	F	30	+	20/20;20/20	Mild macular pigmentary mottling
IV:6	F	22	+	20/20;20/20	Mild macular pigmentary mottling
IV:1	M	39	+	20/40;20/25	Peripheral pigment clumping with macular RPE atrophy
IV:2	M	34	+	20/20;**20/100**	Peripheral pigment clumping with macular RPE atrophy
IV:3	M	32	+	20/20;20/20	Peripheral pigment clumping with macular RPE atrophy
IV:4	M	27	+	20/20;20/20	Peripheral pigment clumping with macular RPE atrophy
IV:5	M	39	+	20/20;20/25	Peripheral pigment clumping with macular RPE atrophy
IV:9	M	28	+	20/30;20/25	Peripheral pigment clumping with macular RPE atrophy
IV:10	F	39	NT	20/20;20/20	Normal exam and autofluorescence
IV:11	M	31	NT	20/40;20/30	Normal exam and autofluorescence